Dynamics of Heat Transfer at the Site Kankule

MULENDA MBUTO Adelin[1], KABASELE YENGA-YENGA Albert[1], MAJALIWA MWANDJALOLO Jackson[2] and Katcho KARUME[3]

1. National Pedagogical University (UPN / Kinshasa), P.O.Box 8815, Kinshasa / Binza, D.R. Congo
2. Makerere Univesity, Kampala P.O. Box 7062 Uganda
3. Evangelical University in Africa (U.E.A), P.O. Box 3323, Bukavu, D.R.Congo

Summary
In this work, we wanted to know the behavior of the soils, near the thermal springs, in Kankule in Katana in South Kivu, in terms of heat transfer. We then aimed to determine first the exact solution of the Fourier equation. Then find the constants involved in the geotherms of each site of our study. Also deduce the temperature gradient, for each site, starting from the geotherm of the place. Finally, make a projection of the type of geothermal energy that can be used on each site. To do this work, we then sampled the soil, thermal water and air temperatures at 14 kankule sites that we had identified. This from 2010 to 2014, from 6 a.m. to 2 p.m., three times a week. Soil and water samples taken by site, we made analyzes of the physical and chemical properties of the soil and water of each site. We then made an analytical resolution of the one-dimensional Fourier equation. Thanks to statistical methods, we were able to determine the damping coefficients "d" intervened in each geotherm as well as the coefficient of thermal diffusivity α. Combining the analytical and statistical method, we were able to find the distribution of the temperature gradient for all sites, and the maximum gradient for each site. Finally, we compared the average kankule gradient of 11.7 ° C per 100 meters to the global thermal gradient of 3.3 ° C per 100 meters. This comparison was made in order to see between low, medium or high energy geothermal energy, which could be exploited in Kankule. The exact solution of the Fourier equation we had obtained is $T = T(z, t) = T_a + A_0 e^{-\frac{z}{d}} \sin\left[\frac{2\pi(t-t_0)}{365} - \frac{z}{d} + \frac{3\pi}{4}\right]$. From this geotherm we found the thermal gradient given by $grad(z, t) = -\sqrt{2}\frac{A_0}{d} e^{-\frac{z}{d}} \cos\left(\frac{2\pi(t-t_0)}{365} - \frac{z}{d} + \frac{\pi}{2}\right)$, in general. The differences stand out with the various values of the constants of the geotherm. The average gradient of any Kankule found is 11.7 ° C per 100 meters. A gradient 3.5 times greater than the global average thermal gradient. Exploiting such a gradient per site, we can exploit different geothermal energy in Kankule: low, medium and high energy, as indicated in the table by Lindal, accepted by the Bureau of Geological and Mining Resources (BRGM, in acronym)
Keywords: *Geothermal or Integral curve and Geothermal gradient*

I. Literature Review

The problem of the electric energy deficit in the DRC is becoming a recurring problem which the National Electricity Company "SNEL" is facing to serve its customers [SNEL, March 29, 2018]. This had led the Congolese parliament to vote on May 13, 2013 on the article on the liberalization of the electricity sector. But the problem remains, because SNEL still retains a monopoly in the marketing of electrical energy, and its services suffer from the numerous load shedding observed to date. Despite that the DR Congo has a high hydroelectric potential, as Jolien Schure et al. [2011]. Thus the dam like Inga operates only at 40% of its capacity, and most of its production is exported instead of serving national needs. In addition, the National Electricity Company (SNEL) is experiencing great difficulties in maintaining facilities for the production, transport and distribution of electricity. The rate of access to electricity in the country is estimated at an average of 6%, 1% for rural areas and 30% for urban areas (Democratic Republic of Congo 2006, Société Nationale d'Electricité [SNEL, Kisangani The consequence is then The wood energy sector occupies an increasingly important place in the DRC The reasons which explain this trend are: the demographic growth of the populations in the big cities, the deterioration of the existing hydro energy infrastructures, the lack of access to other forms of energy, the extreme poverty of the population seeking a means of subsistence, the weakness in the application of forestry legislation and a reforestation policy for unsustainable energy purposes [Jolien Schure et al.]. Also in the countryside, only 1% of the population has access to electricity; in the city, the rate is 30%. Nationally, 6% of the population is supplied with electricity, a rate well below the low average of sub-Saharan Africa (24.6%) (DRC, 2007). "[Friedel Hütz-Adams, January 2008]. This situation accentuates the high dependence of the population on biomass energy. The exploitation of other forms of energy could significantly reduce dependence on biomass [Karume, 2006], and

---

allow the Congolese population to always have energy which is an index of development. The more a people is developed, the more it consumes energy [Duncan T, 2000]. South Kivu, in particular the city of Katana is rich in biodiversity with the Kahuzi-Biega Park in the world heritage. However, this biodiversity is threatened by excessive consumption of firewood by a poor population and impoverished by repeated wars [Ministry of ECN-EF, 2006]. This province has an unexploited geothermal potential which, once developed, would encourage increased investment and job creation [MEM, 1999]. This state of affairs is an urgent necessity to stimulate economic growth and alleviate poverty in the region and the environment. The increase in the population and its demand for energy in the area, requires that we think of other alternatives. Other than hydroelectric which demonstrates its limits to the way of serving the population. Different types of exploitation of the geothermal potential, which take into account environmental requirements are then to be examined. Their management and evaluation are essential [Adelin Mulenda, 2013]. This study seeks to answer the question of How to determine the geothermal potentials of Kankule, for a possible exploitation in electrical energy.

It is therefore important to find the temperature gradient, heat transfer, usable at Kankule in Katana in South Kivu:
- by modeling the shape of the geothermal wave of the sites studied;
- by finding the solution to the Fourier equation, heat transfer, by site by determining the constants involved;
- by determining the temperature gradient per site and;
- by identifying economic holdings.

In thermo-statistics, we gather a set of physical phenomena of movement of molecules in fluids or solids in transport phenomena [Alonso et al, 1986, Alonso et al, 1977, Frederick Reif, 1989]. In the simplest case the equation of the transport phenomenon is of the form: $\frac{\partial \xi}{\partial t} = a^2 \frac{\partial^2 \xi}{\partial x^2}$ (1.1) ,

where a is a constant characteristic of each physical situation and ξ is a quantity corresponding to the particular phenomenon of transport studied like the diffusion of the molecules, the viscosity and the conduction of heat. In this work, we will focus on the last case of these types of transport phenomena whose mathematical solutions relate to a temperature distribution. This phenomenon for heat is described by the Fourier equation which we will solve for a spatial dimension before modeling this solution for the site of Kankule IV. The solution to this equation is called the geotherm.

The Fourier equation for the conduction of heat in the ground, when this energy varies as a function of time t and depth z is: $\frac{\partial^2 T}{\partial z^2} - \frac{1}{\alpha} \frac{\partial T}{\partial t} = 0$ (1.2)

[CER, 2007; Antoine J.P, 2001 - 2002; Gisclon M, 1998 & Lavrentier M et al, 1972; Jean-Paul Barrand et al, 1993; Srishti D. C, 1998]

α being the coefficient of thermal diffusivity of the soil, z the depth and T the temperature characterizing the heat transported.

With the boundary conditions of first species (Dirichlet problem), where the surface temperature is known at all times, this equation admits a sinusoidal solution of progressive wave of the form: $T(z,t) = e^{i(kz - \omega t)}$ (1.3)

Starting from (1. 3), according to Wu and Nofziger [1999], taking into account the boundary conditions, the previous solution can be written: $T(z,t) = \overline{T_0} + \overline{A_0} . e^{-\frac{z}{d}} \sin \left(\frac{2\pi(t - t_0)}{365} - \frac{z}{d} - \frac{\pi}{2} \right)$ (1.4)

With

$\overline{T_0}$: Average annual soil temperature ,

$\overline{A_0}$: The annual average thermal amplitude

t_0: the "time - lag" where an arbitrary day of the month with the lowest temperature.

Knowing that [JABOYEDOFF M, 1999],

$\sigma = \sqrt{2\alpha t}$ (1.5)

where σ is the "variance" of the data collected (we are talking about the standard deviation here although we talked about variance).

α is the thermal diffusivity of the soil

t is the time measured during the same period as ω.

Consequently,

$d = \sqrt{\frac{2\alpha}{\omega}} = \frac{\sigma}{\sqrt{\omega t}} = \frac{\sigma}{\sqrt{2\pi}}$ (1.6)

Always starting from (1.3), we got rather as a solution

$T(z,t) = \overline{T_0} + \overline{A_0} . e^{-\frac{z}{d}} \sin \left(\frac{2\pi(t - t_0)}{365} - \frac{z}{d} + \frac{3\pi}{4} \right)$ (1.7)

These solutions (1.4) and (1.7) improve those proposed by [Alonso, 1986; Alonso, 1977].

(1.4) and (1.7) express the dynamics of the propagation of heat at the sites considered. For this article, we are interested in the Kankule IV site. It is from these solutions that we will determine the temperature gradient of our site.

The Fourier equation describing the dynamics of heat propagation has many applications. Alonso-Finn stipulates its exploitation in soil physics and oceanography and Soil physics [Alonso, 1986; Alonso, 1977]. Their solution to the Fourier equation contains our explicit constants. The works of Wu and Nofziger [1999] give the meaning of some of these constants. These researchers give the general solution of equation (1.2), and apply their work to predict the temperature variation in the soil. By knowing the standard deviation σ, of the soil temperatures, we then find: The coefficient of thermal diffusivity α with the relation $\sigma = \sqrt{2\alpha t}$ [CER, 2007; JABOYEDOFF M, 1999] and deduces thedepth of penetration $d = \sqrt{\frac{2\alpha}{\omega}}$ knowing (J. Antoine, 2001 - 2002). R. Lemmela and Y.Suckdorf [R.Lmmela and Y.Suckdorf, 1981], rather exploit the particular solution suggested by Alonso. However, they specify how to find the constants in the geotherm. In order to be able to produce electricity, the temperature gradient of the study site will have to be exploited. Karim's work [Karim Bédard et al., 2016] exploits this principle well for the sedimentary basin of the Lowlands, in Canada. In this work, the authors have used temperature correction methods, taken from them. They are being corrected by thinking of increasing the thickness of faults, the deep resources of warm water. These waters, which rise by convection, keep almost the same temperature as areas where they were warmed. The Geoscience review of March 16, 2013, shows the operating conditions of geothermal energy to produce electricity. Having active tectonic or volcanic zones in which a surface heat source makes it possible to have a geothermal fluid at a temperature sufficient to produce electricity [Géosciences, 2013]. On page 14, Figure 8, already shows that with a temperature of 50 ° C at 1 km deep, we can consider the production of electricity. It will then be necessary to dig for this to more than 3 km deep. In order to trap the geothermal fluid at more than 150 ° C. The same article presents a world map where high energy geothermal energy is likely to be exploited. Eastern DR. Congo is there, as in all the countries of the Albertine Rift (or Valley). From the ground temperature down to 90 ° C, electricity can already be produced [Ecorem s.a, 2011].

The latest study distinguishes between surface and deep geothermal energy as follows:
- <30 ° C and <500m: surface geothermal energy. This takes up the very low temperatures (enthalpy).
- between 25-30 ° C and 150 ° C and> 500m: deep geothermal energy. This takes over the low and medium temperatures (enthalpy).

Still the same study, specifies that if the geothermal reservoir reaches a temperature above 150 ° C and is encountered at shallow depths, the resource must therefore be in a region where the geothermal gradient is normal (~ 30 ° C / km) or beyond normal. This for the production of electricity. This classification is consistent with that suggested by Lindal for France [Wikipedia, 2020].

The exploitation of high energy geothermal energy is favorable in areas which know geodynamic contexts, showing some form of volcanism. At these points, a significant part of the internal energy of the globe is released. The history of mountain chain formations and terrestrial magmatism allows us to understand the genesis of magma chambers. The latter are foci, zones with strong thermal gradient [J-P Boden et al., 1988]

II.Methodology
For this work, our methodology approach was as follows:
2.1. Description of the study environment
2.1.1. Geographical location of the environment
Our field of study is the locality of Kankule which is located between the latitudes South - 2.241666 ° and - 2.249166 °, East longitude 28.834833 ° and 28.8415 ° and altitude varying between 1565.42 m and 1586 , 44 m.

It is part of the community of Kabare in the South Kivu province of the Democratic Republic of Congo. Kankule is located between the Bidagarha and Lwiro rivers which have their sources in the Kahuzi forest located in the Kahuzi Biega national park, approximately 7 km from our study environment [Adelin M, 2013] and [Bagalwa et alii, 2016]. An image of this site is given in Figure 3.1. below :
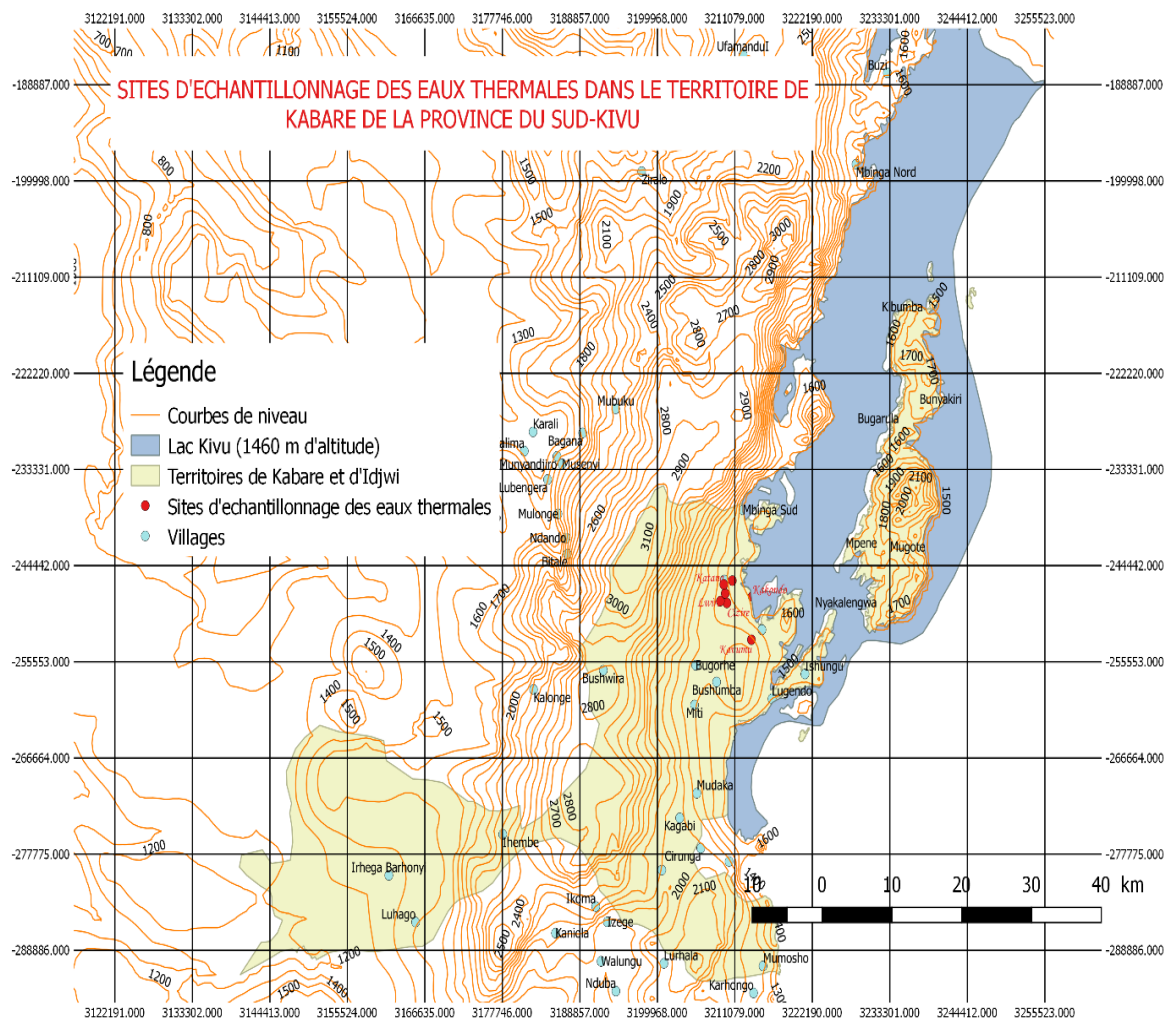
Figure 1: Geolocation of the thermal waters of Kankule, in Katana in South Kivu

2.1.2. Weather

Kankule is located on a part of the chain of Mount Mitumba which spreads over a large part to the east of the Democratic Republic of Congo. The prevailing climate is influenced by this positioning, also its location between Lake Kivu and the Kahuzi Biega National Park. We have a humid tropical climate, tempered by altitude with temperatures ranging from 18 ° C to 22 ° C and rainfall around 1590 mm [PNUD / UNOPS, 1998].

2.1.3. Fauna and vegetation

The fauna is rich in invertebrates and birds which abound in the environment. The flora in some unexploited places remains alpine vegetation, savannas and bamboos, ... in extension of that of the Kahuzi -Biega national park. On the exploited grounds, one finds fields cultivated with predominance of banana plantations and coffee trees,… [PNUD / UNOPS, 1998], beans, cassava, sorghum, quinquinas, tea plants,…

2.1.4. Soil and geology

Located about 7 km from the dormant volcanoes of Kahuzi and Tshibati, the mother rock of Kankule rests on basalts resulting from ancient volcanism and also rests on shales [PNUD / UNOPS, 1998] & [From the geological map of the South Kivu region, 1939]. In the environment abounds in ferrisol (calcite and dolomite of the family of carbonates) and a considerable reserve of travertines, evaluated at 3 million tons in all Katana, raw materials exploited at the cement factory of Katana for the production of cement [UNDP / UNOPS , 1998] with clay and peat also present in quantities not yet evaluated. There are also cold water sources and thermal water sources, the latter of which have greatly contributed to the formation of travertines in the environment [PNUD / UNOPS, 1998] & [From the geological map of the South Kivu region , 1939]. Silica, an important raw material for glassware, is also found on the site. We are here in the presence of a soil important for its physicochemical properties

2.1.5. Population and socio-economic life

The population living in this environment is mainly made up of Bashi who live mainly and mainly from subsistence farming [PNUD / UNOPS, 1998]. The high density in all of Katana is around 300 inhabitants per km² and the growing insecurity around Kankule has seen this density grow strongly year by year, resulting in a strong demand for habitable and cultivable land. There are hardly any heavy industries which would exploit the workforce present in the area to alleviate the misery of the local population who is unable to meet their basic needs [UNDP / UNOPS, 1998].

2.2. Methodological approach

To do this work our methodology was as follows:

2.2.1. Experimental

1 °) From 8h to 14h, with the ground thermometer, we took samples from 14 sites, called Kankule I, Kankule II,…, and Kankule XIV:

- Soil temperatures at 15 cm depth, every day, in 52 weeks To exploit the holographic principle on a macroscopic scale. This principle stipulates that "the information contained on the surface is not less than that contained in volume" [Research, 2009]. This is to find a mechanism to reduce the cost of exploring geothermal energy;

- The temperatures of the thermal waters, during the same period from September 2010 to December 2014. In order to see if the temperature of these waters depends on the study site.

- Ambient air temperatures, at most 2m above the ground. This is to understand the interdependence between the temperatures of the thermal waters, the soil and the surrounding air.

2 °) With a GPS, Garmin brand, we had taken, the geographical coordinates of each site to find the geomagnetic fields of each site, on the NOAA web site

3 °) Excel, R or SPSS software; allowed to determine the constants that intervened in the geotheme (or solution of the Fourier equation) as reported by CER 2OO7 and Wu and Nofziger 1999. This facilitated the temperature gradient distribution analysis that we had obtained.

2.2.2. Analytic

- Solve the Fourier equation in one dimension, to determine the general solution (geotheme), of each site studied.
- Deduce from each geotheme the temperature gradient function per site.
- From the gradient function per site, determine algebraically where geometrically, the maximum gradient per site
- Compare the experimental gradient we obtained with the "theoretical thermal gradient". The latter obtained thanks to the geotheme given by Wu and Nofziger, which is more precise than that suggested by Alonso and Finn (1986).
- Deduct from the average value, from the maximum gradient of the 14 Kankule sites, the depth that can be dug in order to generate electricity.

Indeed ; starting from the one-dimensional Fourier equation: $\frac{\partial^2 T}{\partial z^2} - \frac{1}{\alpha}\frac{\partial T}{\partial t} = 0$:

Wu and Nofziger had found the solution: $T(z,t) = \overline{T_0} + \overline{A_0}\,.e^{-\frac{z}{d}}\sin\left(\frac{2\pi(t-t_0)}{365} - \frac{z}{d} - \frac{\pi}{2}\right)$

Our study rather leads to the result: $T(z,t) = \overline{T_0} + \overline{A_0}\,.e^{-\frac{z}{d}}\sin\left(\frac{2\pi(t-t_0)}{365} - \frac{z}{d} + \frac{3\pi}{4}\right)$

Using these solutions, we looked for the gradient, for each site, with the relation $\partial T / \partial z = f(z)$.

- Then we determined the maximum value of this temperature gradient. First using the solution from Wu and Nofziger. Then we determined the maximum value of this gradient for the solution we obtained. Finally, a comparative study of the distributions of temperature gradients was made.

2.2.3. Statistics

With the results obtained, we checked:

- If there is independence of the soil temperature with the site studied, using the independence test. It is then checked whether the temperature of the thermal waters depended on the study site.

- If the experimental Kankule thermal gradient of 0.117 ° C / m is equivalent to the global average thermal gradient of 0.033 ° C / m; using the compliance test. Here we made the comparison of the 2 means. In order to check whether the gradient of our sites is normal or not.

- If the distribution of our maximum theoretical gradients follows the normal Laplace-Gauss law. Here we carried out the convergence test. This convergence makes it possible to pass from a discrete distribution to a continuous distribution of the temperature gradient; with its probabilistic implications.

- If the distribution of our maximum experimental gradients follows the normal Laplace-Gauss law. Here we also performed the convergence test

- If the distribution of our maximum theoretical gradients and the experimental one are the same, by comparing their:

1) average using the compliance test;

2 °) variance thanks to the homoscedasticity test (or analysis of variances).

This is to be able to check whether the two temperature gradient distributions are identical or not.

2.2.4. Comparison of temperature gradient distributions

 We have proceeded:

- 1 ° to the Comparison of the results of the "theoretical maximum gradient" obtained from the solution of Wu and Nofziger with that which we had obtained, and which we had called experimental. This in order to see the solution to be adopted for the one-dimensional Fourier equation.

- 2 °) to identify how deep we can descend in order to be able to do high or very high energy geothermal energy, for the production of electricity. Compared to what is done elsewhere in the world.

III.Results And Analysis

3.1. Theoretical solution of Wu and Nofziger of the one-dimensional Fourier equation and its normality

3.1.1. Theoretical solution of the Fourier equation

Using the Fourier equation, Wu and Nofziger came to solution (1.4).

This geotherm gives for Kankule IV the figure 2 below. Showing the temperature distribution over time.
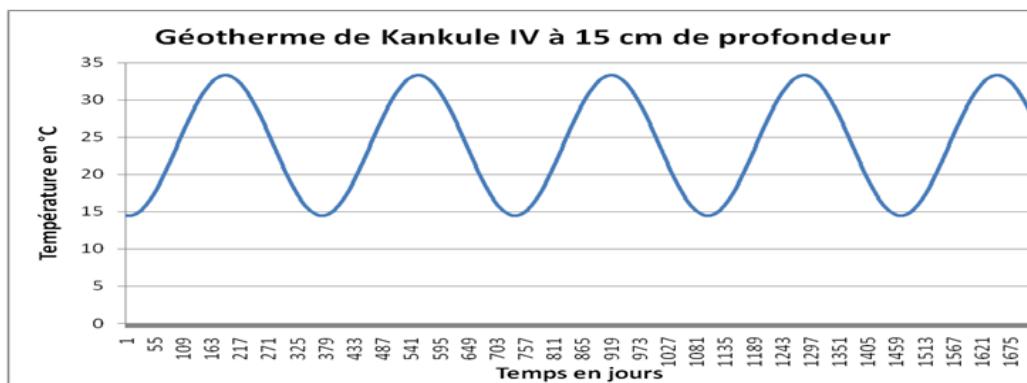

Figure 2: Temperature variation as a function of time for Kankule IV

This same geotherm (1.4), exploited as a function of the depth gives us the curve of figure 3. Indicating the variation of the temperature with the depth on the site of Kankule IV
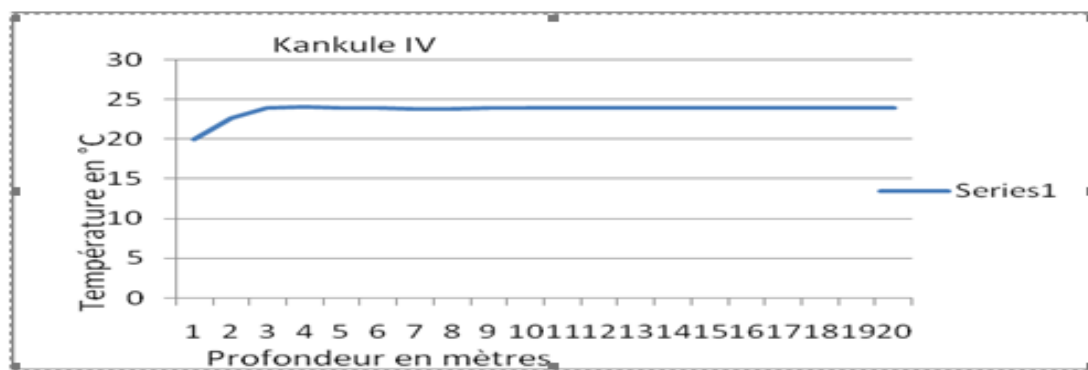

Figure 3: Variation of temperature as a function of depth for Kankule IV

This figure shows that the thermal wave is amortized on a specific date

It just happens that the temperature gradient on a fixed date $(t - t_0)$ is:

grad (z,t) = $-\sqrt{2} \frac{A_0}{d} e^{-\frac{z}{d}} \cos(\frac{2\pi(t-t_0)}{365} - \frac{z}{d} - \frac{3\pi}{4})$ (3.1)

In others words f(z) = $\frac{\partial T}{\partial z}$ = $- \frac{A_0}{z} e^{-\frac{z}{d}} \sin[\frac{2\pi(t-t_0)}{365} - \frac{z}{d} - \frac{\pi}{2}] - \frac{A_0}{z} e^{-\frac{z}{d}} \cos[\frac{2\pi(t-t_0)}{365} - \frac{z}{d} - \frac{\pi}{2}]$. A function that various with the depth z

Let's determine the maximum values of this function, using differential calculus. It comes at a given depth

$$f(z) \neq 0 \quad \begin{cases} -\dfrac{A_0}{z} e^{-\frac{z}{d}} \sin\left[\dfrac{2\pi(t-t_0)}{365} - \dfrac{z}{d} - \dfrac{\pi}{2}\right] - \dfrac{A_0}{z} e^{-\frac{z}{d}} \cos\left[\dfrac{2\pi(t-t_0)}{365} - \dfrac{z}{d} - \dfrac{\pi}{2}\right] \neq 0 \\ \{f'(z) = 0 \Leftrightarrow \{ \quad\quad 2\dfrac{A_0}{d^2} e^{-\frac{z}{d}} \cos\left[\dfrac{2\pi(t-t_0)}{365} - \dfrac{z}{d} - \dfrac{\pi}{2}\right] = 0 \\ f''(z) < 0 \quad\quad 2\dfrac{A_0}{d^3} e^{-\frac{z}{d}} \left(\sin\left[\dfrac{2\pi(t-t_0)}{365} - \dfrac{z}{d} - \dfrac{\pi}{2}\right] - \cos\left[\dfrac{2\pi(t-t_0)}{365} - \dfrac{z}{d} - \dfrac{\pi}{2}\right]\right) < 0 \end{cases}$$

$$f(z) = \dfrac{A_0}{z} e^{-\frac{z}{d}} \neq 0$$

$$\Leftrightarrow \{ \begin{cases} \dfrac{2\pi(t-t_0)}{365} - \dfrac{z}{d} - \dfrac{\pi}{2} = (2k+1)\dfrac{\pi}{2} \; ; with \; k \in \mathbb{z} \quad\quad (3.2) \\ sin(2k+1)\dfrac{\pi}{2} < 0 \end{cases}$$

With z / d> 0, the first value of z which makes the gradient maximum, is obtained for k = -1.
We then find the following results for the Kankule IV site: (Abscissa of the maximum) z = d 60π / 365 = 0.527398921 m and the maximum gradient f (z) = ∂T / ∂z = 6.368167457 ^{0}C / m   (3.3).
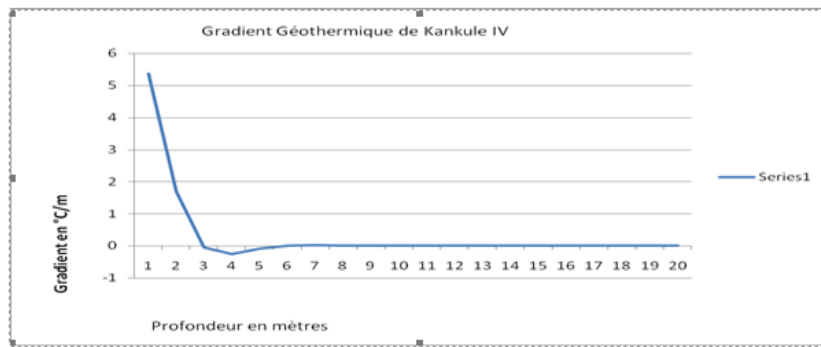The curve from (3.1), for Kankule IV, gives the graph below:

Figure 4: Variation of the Kankule IV temperature gradient as a function of depth z

3.1.2. Normality of the theoretical gradient obtained
For our 14 Kankule sites, the maximum theoretical gradients are given in table 1, below:

Table 1: Maximum gradient per Kankule site, with the Wu and Nofziger model of the geotheme (1.4)

	KANK ULE I	KANK ULE II	KANK ULE III	KANK ULE IV	KANK ULEV	KANK ULE VI	KANK ULE VII	KANK ULE VIII	KANK ULE IX	KANK ULE X	KAN KUL E XI	KANK ULE XII	KANK ULE XIII	KAN KUL E XIV
Maximu mGradien t (°C /m)	4.7805 55514	6.3785 25961	4.9734 81366	6.3681 67457	6.669 04952	4.228 52612	5.887 87759	6.5228 30499	6.161 31247 5	6.7169 07666	6.90 8516	5.4637 91034	4.8254 24153	7.27 8536

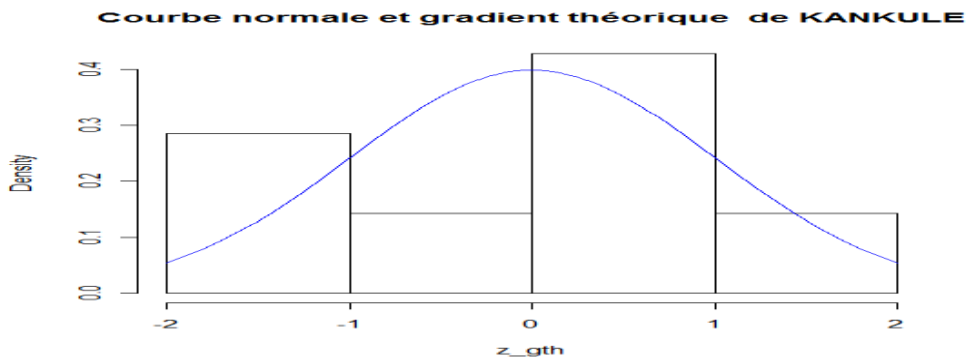The normality test of these values gives the following results:

Figure 5: Normality test of the theoretical gradient with the Gaussian curve

The temperature gradient distribution histogram is close to the normal blue Laplace-Gauss curve
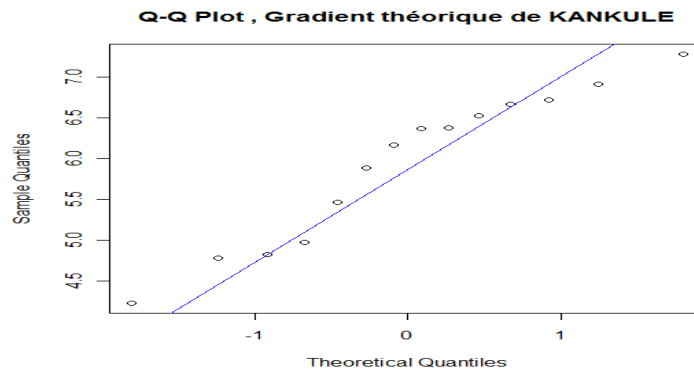

Figure 6: Normality test with Q-Q Plot and Henry's line

The cloud of temperature distribution points is close to the right of Henry
shapiro.test (grad_theorique)
    Shapiro-Wilk normality test
data: grad_theorique
W = 0.9342, p-value = 0.349
We see that at the probability threshold of $\alpha = 0.05$, p-value = 0.349 is greater than 0.05. So we accept the null hypothesis of normality of our temperature gradient distribution.
These 3 tests express that the theoretical gradient follows the normal Laplace-Gauss law.

3.2. Analytical solution of the one-dimensional Fourier equation and its normality
3.2.1. Analytic-experimental solution of the one-dimensional Fourier equation
The solution of the Fourier equation that we obtained, analytically, is the geotherm (1.7). Its representative curve, as a function of time, at a fixed depth of 15cm, gives for Kankule IV the figure below:
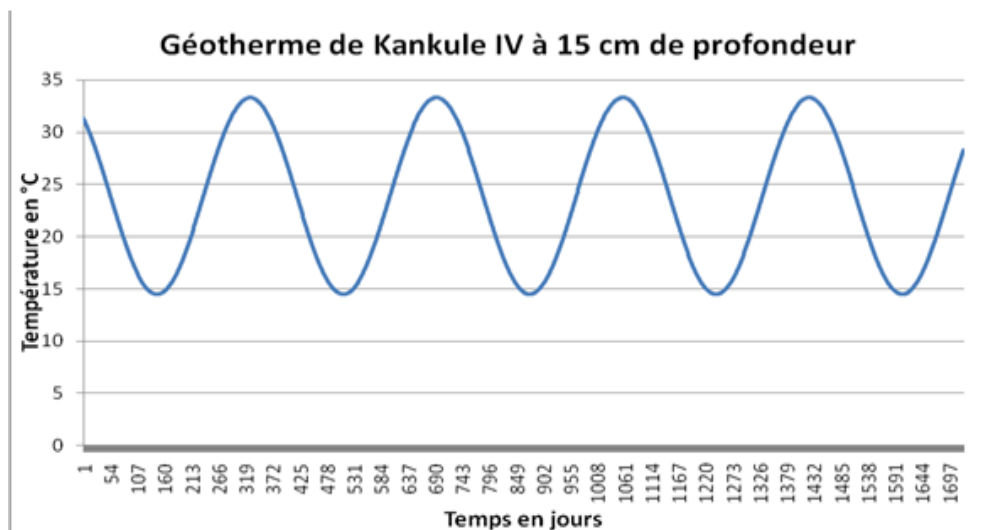

Figure 1.7: Analytical geotherm obtained for Kankule IV

This result is similar to that of figure 1.2, with a shift of the sinusoid extremes. We also obtain a curve similar to that of FIG. 3, for the thermal wave. What about the temperature gradient then?
Calculations analogous to those of paragraph 4.1, allowed us to obtain the following gradient:

$$\text{grad } (z,t) = -\sqrt{2}\frac{A_0}{d} e^{-\frac{z}{d}}\cos(\frac{2\pi(t-t_0)}{365} - -\frac{z}{d}+\frac{\pi}{2}) \qquad (3.4).$$

Is $g (z) = \frac{\partial T}{\partial z}z = -\frac{A_0}{z} e^{-\frac{z}{d}} \sin [\frac{2\pi(t-t_0)}{365} - \frac{z}{d} + \frac{3\pi}{4}] - \frac{A_0}{z} e^{-\frac{z}{d}} \cos [\frac{2\pi(t-t_0)}{365} - \frac{z}{d} + \frac{3\pi}{4}]$,
a function that varies with depth z.

Let's determine the maximum values of this function, using differential calculus. It comes at a given depth

$$g(z) > 0$$
$$\{g'(z) = 0 \Leftrightarrow \{$$
$$g''(z) < 0$$

$$-\frac{A_0}{z}e^{-\frac{z}{d}}\left(\sin\left[\frac{2\pi(t-t_0)}{365} - \frac{z}{d} + \frac{3\pi}{4}\right] + e^{-\frac{z}{d}}\cos\left[\frac{2\pi(t-t_0)}{365} - \frac{z}{d} + \frac{3\pi}{4}\right]\right) > 0$$

$$2\frac{A_0}{d^2}e^{-\frac{z}{d}}\cos\left[\frac{2\pi(t-t_0)}{365} - \frac{z}{d} + \frac{3\pi}{4}\right] = 0$$

$$2\frac{A_0}{d^3}e^{-\frac{z}{d}}\left(\sin\left[\frac{2\pi(t-t_0)}{365} - \frac{z}{d} + \frac{3\pi}{4}\right] - \cos\left[\frac{2\pi(t-t_0)}{365} - \frac{z}{d} + \frac{3\pi}{4}\right]\right) < 0$$

$$g(z) = \frac{A_0}{z}e^{-\frac{z}{d}} > 0$$

$$\Leftrightarrow \{\frac{2\pi(t-t_0)}{365} - \frac{z}{d} + \frac{3\pi}{4} = (2k+1)\frac{\pi}{2} \ ; with \ k \in \mathbb{z} \quad (3.5)$$

$$\sin(2k+1)\frac{\pi}{2} < 0$$

With $z / d > 0$, the first value of z which makes the gradient maximum, is obtained for k = -1.
We then find the following results for the Kankule IV site:
(Abscissa of the maximum) z = d * π (1.25 + 60/365) = 4.537828208 m and the maximum gradient g (z) = $\partial T / \partial z$ = 0.125471195 ^{0}C / m   (3.6). What can be seen in the figure below:
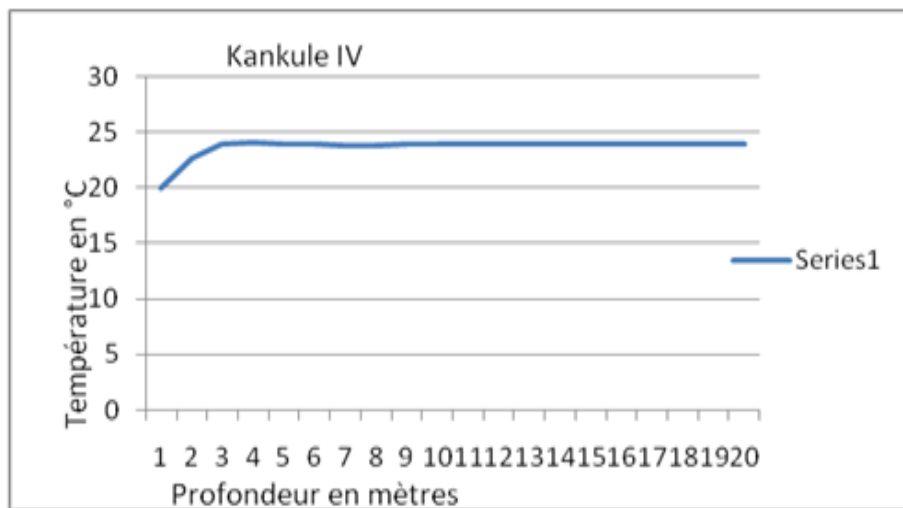

Figure 1.8: Variation of the Kankule IV temperature gradient with the depth z

This gradient obtained is a reflection of the experimental results in situ, through thermal waters. It is a gradient 3.5 times greater than the average continental gradient of 0.033 ° C / m.

3.2.2. On the normality of the analytical-experimental gradient
Starting from solution (3.4), we find for our 14 Kankule sites, the maximum gradients that we present in the following table:

Table 2: Maximum gradient of the 14 Kankule sites starting from our geotherm (1.7)

	KAN KUL E I	KAN KUL E II	KAN KUL E III	KAN KUL E IV	KAN KUL E V	KAN KUL E VI	KAN KUL E VII	KAN KUL E VIII	KAN KUL E IX	KAN KUL E X	KAN KUL E XI	KAN KUL E XII	KAN KUL E XIII	KAN KUL E XIV
gradient (maximum (°C / m)	0,094 1906 79	0,125 6752 88	0,097 9918 72	0,125 4711 95	0,131 3994 37	0,083 3141 14	0,116 0081 05	0,128 5185 02	0,121 3955 58	0,132 3423 8	0,136 118		0,095 0747 2	0,143 408

Comparing this experimental temperature gradient distribution to the normal Laplace-Gauss law, we statistically obtained the following results:
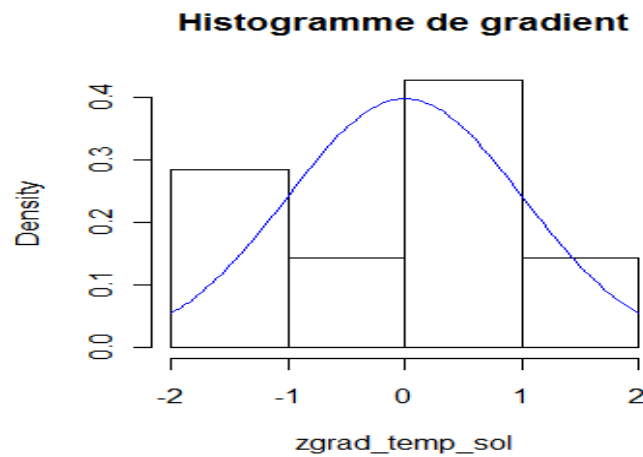
Histogramme de gradient

Figure 9: Test of normality of the experimental gradient with the Gauss curve

We observe that the histogram, of experimental temperature gradient distribution, is close to the blue, normal Laplace-Gauss curve. We then agree that the theoretical temperature gradient distribution follows the normal law
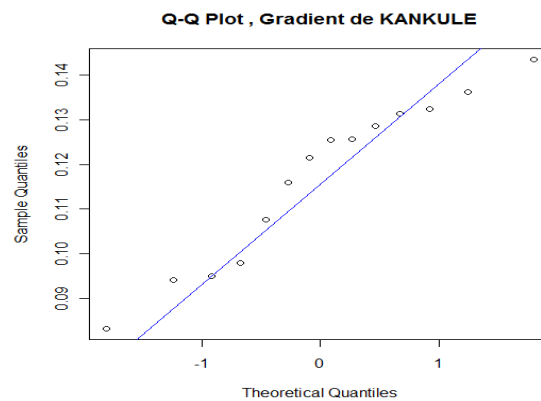

Figure 10: Q-Q Plot and Henry's line of experimental temperature gradient

Same observation as in analogous figure 1.6

The Shapiro-Wilk test gives us the result below:

> shapiro.test (grad_temp_sol)

  Shapiro-Wilk normality test

data: grad_temp_sol

W = 0.9342, p-value = 0.349

3.3. On the independence of temperatures with the sites

Wanting to know if the temperatures sampled in situ depend on the study site, we then carried out the independence test. The results are given below:
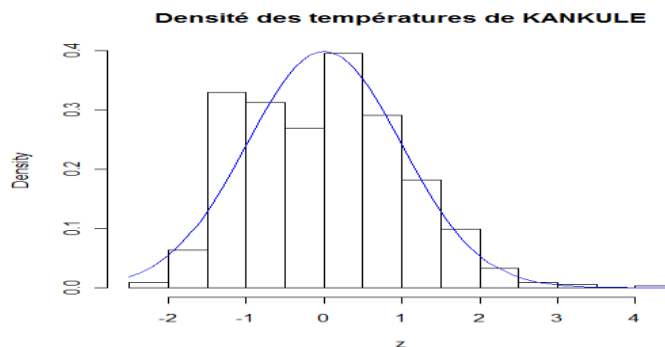

Figure 11: Normality of temperature distribution

This graph shows us that the distribution of the temperatures taken follows the normal law.

The independence test, gave us the following result, with the R software:

Table 3: ResuElt of the temperature independence test with the study site

> summary (model)

	Df	Sum Sq	Mean Sq	F value	Pr(>F)	
data_indep$Site	13	25326.1	1948.2	83.521	< 2.2e-16	***
Residuals	714	16654.3	23.3			

Significant. codes: 0 '***' 0.001 '**' 0.01 '*' 0.05 '.' 0.1 ' ' 1

3.3.3. On the conformity of the Kankule temperature gradient

Wondering if the average experimental Kankule thermal gradient, which gives m = 0.117 [° C / m], if it is equal to the global average thermal gradient of mo = 0.033 [° C / m]; we carry out the comparison test of the means below, in R:

> t.test (grad_temp_sol, mu = 0.033)

    One Sample t-test

data: grad_temp_sol

t = 17.1116, df = 13, p-value = 2.692e-10

alternative hypothesis: true mean is not equal to 0.033

95 percent confidence interval:

0.1064298 0.1276502

sample estimates:

mean of x

0.11704

3.3.5. The homogeneity of the theoretical gradient and the experimental Kankule gradient.

The comparison of the means of the maximum gradients, obtained with the theoretical formula of Wu and Nofziger and that which we had obtained analytically and experimentally; we get the results below:

> t.test (grad_temp_sol, grad_theorique)

Welch Two Sample t-test

data: grad_temp_sol and grad_theorique

t = -23.3567, df = 13.01, p-value = 5.243e-12

alternative hypothesis: true difference in means is not equal to 0

95 percent confidence interval:

 -6.361783 -5.284637

sample estimates:

mean of x mean of y

0.11704 5.94025

This result means that the means of the gradients obtained, with the theoretical gradient and the experimental gradient, are not the same. We therefore reject the null hypothesis of equality of the means of these two distributions. Which brings us to check if the two distributions are identical, by comparing their variances

3.3.6 Homoscedasticity of the two distributions

The Anova test, on the variances of distribution of the theoretical and experimental maximum gradients, we obtain the results below, with software R:

var.test (grad_temp_sol, grad_theorique)

    F test to compare two variances

data: grad_temp_sol and grad_theorique

F = 4e-04, num df = 13, denom df = 13, p-value <2.2e-16

alternative hypothesis: true ratio of variances is not equal to 1

95 percent confidence interval:

0.0001246224 0.0012092669

sample estimates:

ratio of variances

    0.0003882032

IV.Discussion Of The Results

1) Is the average experimental Kankule thermal gradient, which gives m = 0.117 [° C / m], equal to the global average thermal gradient of m_o = 0.033 [° C / m]? The temperature gradient compliance test, in paragraph 3.3, rejects this assumption at the threshold of 0.05. This test accepts the alternative hypothesis, which implies that the thermal gradient depends on the study site. Adelin MULENDA, 2013, already finds that the temperature of thermal waters depends on that of the soil of the study site. And the intensity of this dependence is 58.8%. Results which implied that the physico-chemical properties of the soil of the study site had also influenced the temperature of the thermal waters.

2) Do the solutions (1.4) and (1.7) of (1.2) reflect the same physical reality? We can observe that these solutions present similarity and dissimilarity. Figures 1 and 6 show two sinusoids, one translation of the other. This in terms of temperature variation depending on the site studied. Figures n ° 5 or 8, as well as n ° 9 or 10 reinforce this resemblance. This in terms of convergence to the normal law, temperature gradient distributions resulting from (1 .4) via (3 .1) and from (1.3) via (3.4). On the other hand, the tables of temperature gradients, obtained in paragraphs 4 .1. and 4.2., show that the temperature gradient distributions, from (1.4) and (1.7), are not the same. Figures 4 and 8 illustrate this dissimilarity in temperature gradient distribution. What about the temperature gradient distribution around their mean value; with these two distributions? The homogeneity test, in section 4.3.5, further demonstrates that the temperature gradient distributions, resulting (1.4) and (1.7), are not identical. Consequently one of the solutions of the Fourier equation (1.2), here (1.4) or (1.7), will have to be retained and the other rejected. Since for a differential equation, with the conditions of Cauchy and Dirichlet, the solution is unique. Let us then analyze which solution should be retained.

3) Let us carry out the comparative study of the two temperature gradient distributions as a function of the realities observed in situ. With solution (1.4), we arrive at an average gradient of 5.94 ° C / m.

The theoretical gradient which gave us an average of 5.94 ° C / m at shallow depth, should allow thermal waters, taken at least 100m deep, to have temperatures above 594 ° C. This situation is therefore not observed on land, where these waters have maximum temperatures of 75 ° C. To have such temperatures, the water sources should be 11m deep. This in accordance with [Adelin, 2013], which gives:

$$T_{water} = 43.789 + 0.481 \, T_{soil} \qquad (4.1)$$

This implies that water sources, like Bidagarha, from at least 5 m deep would be hot. What is not observed on the ground because these waters on the ground surface with temperatures of less than 15 ° C. On the other hand, the solution (1.7) gives an average thermal gradient of 0.117 ° C / m. This is consistent with the surface temperature of the Bidagarha source, which is below the ambient air temperature. This gradient of 0.117 ° C / m also helps to understand the abundance of travertine in this area. This raw material of cement results from the formation of stalactites and stalagmites, at a temperature of less than 15 ° C [Robers J and al, 1998]. Thus cold water sources, circulating even at a depth of 100m, will not have a temperature of 12 ° C. In view of these observations, we then reject solution (1.4) obtained by Wu and Nofziger. For equation (1.2), we only retain solution (1.7). The analysis carried out in paragraph (4.3.6), also led us to reject the solution that Wu and Nofziger use for the Fourier heat transfer equation (1.2).

4)Which of the geotherms (1.4) and (1 .7) verify (1.2)?

To find out, we then introduce these results into equation (1.2) and see more

For equation (1.2) for which Wu and Nofziger find the solution

$$T = T(z, t) = T_a + A_0 e^{-\frac{z}{d}} \sin\left[\frac{2\pi(t-t_0)}{365} - \frac{z}{d} - \frac{\pi}{2}\right] (1.4), \text{ with } d = \sqrt{\frac{2\alpha}{\omega}} \text{ and } \omega = 2\pi / 365$$

He then comes

$$(1*) \ T_t''(z;t) = \frac{1}{\alpha}\frac{\partial T}{\partial t} = \frac{1}{\alpha}\frac{2\pi}{365}A_0 e^{-\frac{z}{d}} \cos\left[\frac{2\pi(t-t_0)}{365} - \frac{z}{d} - \frac{\pi}{2}\right]$$

$$= \frac{A_0}{\alpha}\omega e^{-\frac{z}{d}} \cos\left[\frac{2\pi(t-t_0)}{365} - \frac{z}{d} - \frac{\pi}{2}\right] (4.2)$$

$$(2*) \ T_z''(z;t) = \frac{\partial^2 T}{\partial z^2} = \frac{\partial}{\partial z}\left(\frac{\partial T}{\partial z}\right)$$

$$= \frac{\partial}{\partial z}\left[-\frac{A_o}{d}e^{-\frac{z}{d}}\sin\left(\frac{2\pi(t-t_o)}{365} - \frac{z}{d} - \frac{\pi}{2}\right) - \frac{A_o}{d}e^{-\frac{z}{d}}\cos\left(\frac{2\pi(t-t_o)}{365} - \frac{z}{d} - \frac{\pi}{2}\right)\right]$$

$$= -\frac{A_o}{d}\frac{\partial}{\partial z}\left[e^{-\frac{z}{d}}\left(\cos\left(\frac{2\pi(t-t_o)}{365} - \frac{z}{d} - \frac{\pi}{2}\right) - \cos\left(\frac{2\pi(t-t_o)}{365} - \frac{z}{d}\right)\right)\right]$$

$$= \frac{2A_o}{d}\frac{\partial}{\partial z}\left[e^{-\frac{z}{d}}\sin\left(\frac{2\pi(t-t_o)}{365} - \frac{z}{d} - \frac{\pi}{4}\right)\sin\left(-\frac{\pi}{4}\right)\right]$$

$$= -\frac{\sqrt{2}}{d}A_o\frac{\partial}{\partial z}\left[e^{-\frac{z}{d}}\sin\left(\frac{2\pi(t-t_o)}{365} - \frac{z}{d} - \frac{\pi}{4}\right)\right]$$

$$= -\frac{\sqrt{2}}{d}A_o\left[-\frac{1}{d}e^{-\frac{z}{d}}\sin\left(\frac{2\pi(t-t_o)}{365} - \frac{z}{d} - \frac{\pi}{4}\right) - \frac{1}{d}e^{-\frac{z}{d}}\cos\left(\frac{2\pi(t-t_o)}{365} - \frac{z}{d} - \frac{\pi}{4}\right)\right]$$

$$= \frac{\sqrt{2}}{d^2}A_o e^{-\frac{z}{d}}\left[\sin\left(\frac{2\pi(t-t_o)}{365} - \frac{z}{d} - \frac{\pi}{4}\right) + \cos\left(\frac{2\pi(t-t_o)}{365} - \frac{z}{d} - \frac{\pi}{4}\right)\right]$$

$$= \frac{\sqrt{2}}{d^2}A_o e^{-\frac{z}{d}}\left[\sin\left(\frac{2\pi(t-t_o)}{365} - \frac{z}{d} - \frac{\pi}{4}\right) + \sin\left(\frac{2\pi(t-t_o)}{365} - \frac{z}{d} - \frac{\pi}{4} + \frac{2\pi}{4}\right)\right]$$

$$= \frac{\sqrt{2}}{d^2} A_o e^{-\frac{z}{d}} \left[\sin \left(\frac{2\pi (t - t_o)}{365} - \frac{z}{d} - \frac{\pi}{4} \right) + \sin \left(\frac{2\pi (t - t_o)}{365} - \frac{z}{d} + \frac{\pi}{4} \right) \right]$$

$$= \frac{2}{d^2} A_o e^{-\frac{z}{d}} \sin \left(\frac{2\pi (t - t_o)}{365} - \frac{z}{d} \right)$$

$$= \frac{A_0}{\alpha} \omega e^{-\frac{z}{d}} \sin \left[\frac{2\pi(t - t_0)}{365} - \frac{z}{d} \right] \qquad (4.3)$$

Comparing solutions (4.2) and (4.3), we find that the two results differ. We then conclude that solution (1.4), given by Wu and Nofziger is not suitable as solution of (1.2).

The result that we found for the geotherm being

$$T = T (z, t) = T_a + A_0 e^{-\frac{z}{d}} \sin \left[\frac{2\pi(t - t_0)}{365} - \frac{z}{d} + \frac{3\pi}{4} \right] (1.7), \text{ with } d = \sqrt{\frac{2\alpha}{\omega}} \text{ and } \omega = \frac{2\pi}{365};$$

Then he comes:

$$(*) T'_t (z ; t) = \frac{1}{\alpha} \frac{\partial T}{\partial t} = \frac{1}{\alpha} \frac{2\pi}{365} A_0 e^{-\frac{z}{d}} \cos \left[\frac{2\pi(t - t_0)}{365} - \frac{z}{d} + \frac{3\pi}{4} \right]$$

$$= \frac{A_0}{\alpha} \omega e^{-\frac{z}{d}} \cos \left[\frac{2\pi(t - t_0)}{365} - \frac{z}{d} + \frac{3\pi}{4} \right] \qquad (4.4)$$

$$(2*) \quad T''_z (z ; t) = \frac{\partial^2 T}{\partial z^2} = \frac{\partial}{\partial z} \left(\frac{\partial T}{\partial z} \right)$$

$$= \frac{\partial}{\partial z} \left[- \frac{A_0}{d} e^{-\frac{z}{d}} \sin \left(\frac{2\pi (t - t_o)}{365} - \frac{z}{d} + \frac{3\pi}{4} \right) - \frac{A_0}{d} e^{-\frac{z}{d}} \cos \left(\frac{2\pi (t - t_o)}{365} - \frac{z}{d} + \frac{3\pi}{4} \right) \right]$$

$$= - \frac{A_o}{d} \frac{\partial}{\partial z} \left[e^{-\frac{z}{d}} \left(\sin \left(\frac{2\pi (t - t_o)}{365} - \frac{z}{d} + \frac{3\pi}{4} \right) + \sin \left(\frac{2\pi (t - t_o)}{365} - \frac{z}{d} + \frac{3\pi}{4} + \frac{2\pi}{4} \right) \right) \right]$$

$$= - \frac{2 A_o}{d} \frac{\partial}{\partial z} \left[e^{-\frac{z}{d}} \sin \left(\frac{2\pi (t - t_o)}{365} - \frac{z}{d} + \frac{3\pi}{4} + \frac{\pi}{4} \right) \cos \left(\frac{\pi}{4} \right) \right]$$

$$= - \frac{\sqrt{2}}{d} A_o \frac{\partial}{\partial z} \left[e^{-\frac{z}{d}} \sin \left(\frac{2\pi (t - t_o)}{365} - \frac{z}{d} + \pi \right) \right]$$

$$= \frac{\sqrt{2}}{d} A_o \frac{\partial}{\partial z} \left[e^{-\frac{z}{d}} \sin \left(\frac{2\pi (t - t_o)}{365} - \frac{z}{d} \right) \right]$$

$$= \frac{\sqrt{2}}{d} A_o \left[- \frac{1}{d} e^{-\frac{z}{d}} \sin \left(\frac{2\pi (t - t_o)}{365} - \frac{z}{d} \right) - \frac{1}{d} e^{-\frac{z}{d}} \cos \left(\frac{2\pi (t - t_o)}{365} - \frac{z}{d} \right) \right]$$

$$= - \frac{\sqrt{2}}{d^2} A_o e^{-\frac{z}{d}} \left[\sin \left(\frac{2\pi (t - t_o)}{365} - \frac{z}{d} \right) + \sin \left(\frac{2\pi (t - t_o)}{365} - \frac{z}{d} + \frac{\pi}{2} \right) \right]$$

$$= - \frac{\sqrt{2}}{d^2} A_o e^{-\frac{z}{d}} \left[2 \sin \left(\frac{2\pi (t - t_o)}{365} - \frac{z}{d} + \frac{\pi}{4} \right) \cos \left(- \frac{\pi}{4} \right) \right]$$

$$= - \frac{2}{d^2} A_o e^{-\frac{z}{d}} \sin \left(\frac{2\pi (t - t_o)}{365} - \frac{z}{d} + \frac{\pi}{4} \right)$$

$$= - \frac{A_0}{\alpha} \omega e^{-\frac{z}{d}} \sin \left[\frac{2\pi(t - t_0)}{365} - \frac{z}{d} + \frac{\pi}{4} \right]$$

$$= \frac{A_0}{\alpha} \omega e^{-\frac{z}{d}} \cos \left[\frac{2\pi(t - t_0)}{365} - \frac{z}{d} + \frac{\pi}{4} + \frac{2\pi}{4} \right]$$

$$= \frac{A_0}{\alpha} \omega e^{-\frac{z}{d}} \cos \left[\frac{2\pi(t - t_0)}{365} - \frac{z}{d} + \frac{3\pi}{4} \right] \qquad (4.5)$$

Comparing solutions (4.4) and (4.5), we find that the two results are equal. We then conclude that the relation (1.7), is suitable as solution of (1.2)

This analysis of the solution used by Wu and Nofziger shows that it is not the integral of the one-dimensional Fourier equation (1.2). This is why it has not been exploited by Alonso / Finn [1986]. The result of the latter verifies the Fourier equation. Its only problem is that some constants of the geotheme are not well specified.

5) Is the Kankule thermal gradient normal or not? In other words, is the average experimental Kankule thermal gradient, which gives m = 0.117 [° C / m], equal to the global average thermal gradient of mo = 0.033 [° C / m]? The conformance test, in section 3.4, allows us to see that the average Kankule thermal gradient of 0.117 ° C / m differs from the global average thermal gradient of 0.033 ° C / m. This Kankule gradient is 3.5 times greater than the global average thermal gradient. With this average Kankule thermal gradient, we should be able to exploit different types of geothermal energy as indicated [Ecorem s.a, 2011]. The different types of geothermal energy that can be used in Kankule are:

• <30 ° C and <500m: surface geothermal energy. This takes up the very low temperatures (enthalpy). Because at 257m deep, we will have temperatures of at most 30 ° C

• between 25-30 ° C and 150 ° C and> 500m: deep geothermal energy. Because at a depth of 500m, we will already have a temperature of 58.5 ° C. In order to generate electricity, it would have to be over 100 ° C. By digging up to 1500m, or 1.5km, deep, we will have temperatures reaching 175.5 ° C. Going up to 2000m deep, we will have a temperature of 234 ° C. The production of electricity is then possible from 50 ° C as already pointed out [Géoscience, 2013].

• For Kankule IV, with a gradient of 125, 471195 ° C / km. You can reach desired temperatures by drawing water more than 2 km deep, reaching temperatures of 234 ° C. A good result when we already compare them to that of Soultz in France [SVT, 2019] and [Wikipedia, 2020].

5. Conclusion

Our study made it possible to find the temperature gradient, heat transfer, usable at Kankule in Katana in South Kivu, given by the relation (1.7).

It also made it possible to see that the solution of the Fourier equation of heat transfer, given by Wu and Nofziger, is rejected by what is observed in situ. Knowledge of an exact solution to the Fourier equation was necessary to estimate the geothermal potential that could be exploited at Kankule.

When geothermal water has a temperature of 90 to 160 ° C, it can be used in liquid form in the production of electricity: it is medium energy geothermal energy. If the temperature of geothermal water exceeds 160 ° C, this water can be used directly, in the form of steam, to turn turbines generating electricity: we speak of high energy geothermal energy. For Kankule IV, with a gradient of 125, 471195 ° C / km. You can reach desired temperatures by drawing water more than 2 km deep, reaching temperatures of 234 ° C. A good result when we already compare them to that of Soultz in France. Indeed, in this French site in Alsace, to reach the temperature of 203 ° C, one would have to dig up to 5.01 km deep [SVT, 2019]. And the electric power supplied on this site is 13 MW, including 2, 1 MW of raw electric production [Wikipedia, 2020].

Bibliography

[1]. Adelin Mulenda, 2013, *Modélisation du transfert des températures sol-air-eau thermale de Kankule dans Katana au Sud-Kivu*, Mémoire de D.E.A présenté à l'Université Pédagogique Nationale de Kinshasa (UPN /Kin), Faculté des Sciences, Département de Physique.
[2]. Alonso /Finn et al, 1986, Physique générale 1, Mécanique et thermodynamique, Inter Editions, Paris
[3]. Alonso / Finn et al, 1977, Physique générale 2, Champs et Ondes, Inter Editions, Paris
[4]. Beaujard P et al, 2002, Sciences de la Vie et de la Terre, Enseignement de spécialité, Hatier, Paris
[5]. Cédrick Copol, 2016, Etudes mathématiques et numériques pour la modélisation des systèmes hydrothermaux. Applications à la géothermie haute énergie. Thèse pour obtenir le grade de docteur délivré par l'Université des Antilles. Faculté des Sciences Exactes et naturelles.
[6]. CER, 2007, Revue des Energies Renouvelables, Détermination du champ de Température dans le sol, par un modèle semi-analytiyle. Conditions aux limites pour les besoins de simulation d'une serre de culture, 2007.
[7]. Dumolard P et al, 2003, les statistiques en géographie, Belin, Paris
[8]. Duncan T, 2000, Advanced Physics, Hodder Education, London
[9]. Ecorem s.a, 2011, Etude des obstacles à la géothermie profonde (basse et haute énergie), Rapport final, Département de l'énergie, Wallonie
[10]. Frederick Reif, 1989, Physique statistique, Berkeley : Cours de Physique, volume 5, Armand Colin, Paris
[11]. Friedel Hütz-Adams, January 2008, Energie et Eau en République Démocratiques du Congo, Evangelischer Entwicklungsdienst (EED), Bonn
[12]. Géosciences, 2013, La revue du BRGM pour une Terre durable, n° 16
[13]. Gisclon M, 1998, Le journal de maths des élèves. Volume 1 (1998), n°4 A propos de l'équation de la chaleur et de l'analyse de Fourier
[14]. Howard A, 1995, Calculus, With Analytic Geometry, John Wiley & Sons, New York
[15]. J-P Boden et al.., 1988, Biologie et Géologie, Première S, Bordas, Paris
[16]. JABOYEDOFF M, 1999, Bulletin n°340 des laboratoires de Géologie, minéralogie, géophysique et du musée géologique de l'université de Lausanne, Modèle thermique simple de la croûte terrestre : un regard sur les alpes, Paris
[17]. Jean-François Moyen, Bureau de Recherche Géologique et Minière, Benoît Urgelli
[18]. ENS Lyon / DGESCO, 15/11/2001
[19]. Jean-Paul Barrand et al., 1993, Initiation aux transferts thermiques, Lavoisier TEC & DOC, Paris
[20]. Jolien Schure et al., 2011, Bois énergie en RDC : Analyse de la filière des villes de Kinshasa et de Kisangani ; Projet Makala/CIFOR, Kinshasa
[21]. Karim Bédard et al., 2016, Evaluation des ressources géothermiques du bassin des Basses- Terres du Saint-Laurent, IREQ, Québec
[22]. Katcho Karume, 2006, *Biomass and hydropower potential and demand in Uganda Albertine Rif Region*, PhD Thesis submitted at Makerere University, Physics Department.
[23]. KINNEAR P et al., 2005, SPSS facile appliquée à la psychologie et aux sciences sociales : Maitriser le traitement de données, De Boeck, Bruxelles
[24]. Lavrentier M et al., 1972, Méthodes de la théorie des fonctions d'une variable complexe, Mir, Moscou
[25]. Nofzinger D.I and al., 2003, Soil Temperature change with Time and Depth: Theory
[26]. Pierre Dagnelie, 1988, Théorie et méthodes statistiques, Applications Agronomiques, vol 1, Les Presses Agronomiques de Gembloux
[27]. N Piskounov, 1980, Calcul différentiel et intégral, Mir, Moscou
[28]. R.Lemmela et Y.Suckdorf, 1981, Annual variation of soil temperature at depths 20 to 700 cm in an experimental field in Hyryla, South-Finland during 1969 to 1973, geophysica_1981_17_1_2
[29]. Recherche ; 2009, « L'univers est un hologramme », pp 38-41
[30]. Ricco Rakatomalala, 2001, Tests de normalité, Techniques empiriques et tests statistiques, Université Lumière Lyon 2
[31]. Robers J. et al, 1998, Modern Earth Science, Holt, New York
[32]. Spallanzani A M et al., 2006, Probabilités et statistiques pour la gestion et l'économie, Presse universitaire de Grenoble
[33]. SNEL, 2018, La problématique du déficit énergétique en RDC
[34]. Srishti D. Chatterji, 1998, Cours d'Analyse, 3 Equations différentielles ordinaires et aux dérivées partielles, Presses Polytechniques et universitaires romandes, Lausanne
[35]. S.V.T, consulté le 16 juillet 2019, Correction de la géothermie, Correction_ géothermie –SF-SVT Lyon, pdf
[36]. V .Koudriatsev et al., 1986, Cours élémentaire de mathématiques supérieures, Mir, Moscou
[37]. UN, 2014, Commission économique pour l'Afrique, Accès à l'énergie et sécurité énergétique en Afrique de l'Est Situation actuelle et moyens de l'améliorer, Kigali (Rwanda)
[38]. www.Wikipedia.fr/géothermie , consulté le 19 septembre 2020
[39]. http://www.geothermie-perspectives.fr/05-geothermie/index-html, consulté le 9 janvier 2013
[40]. http://www.geothermie-soultz.fr/ , consulté le 7 septembre 2019

[41].   http://www.iac.ethz.ch/fuhrer/publ/publ/dipl "heat transfert in soil , consulté le 29 août 2013